

Structural rearrangement of solid surfaces due to competing adsorbate-substrate interactions

E. V. Vakarin,^{1,*} A. E. Filippov,^{1,†} J. P. Badiali,^{1,‡} and M. F. Holovko²

¹*Structure et Réactivité des Systèmes Interfaciaux, Université Pierre et Marie Curie, 4 Place Jussieu, 75230 Paris Cedex 05, France*

²*Institute for Condensed Matter Physics, Svientsitsky strasse 1, 290011, Lviv, Ukraine*

(Received 8 October 1998)

Employing a generalized lattice gas theory and the Brownian dynamics simulation, we show that the competing displacive interaction in an adsorbate may cause a continuous distortive transition in the underlying substrate. The threshold for the transition is determined by the competition of the substrate rigidity and the quasielastic energy induced by the adsorbate. In the presence of a strong pinning and repulsive lateral interaction, the resulting structure appears as a compromise between the square lattice of the substrate and the hexagonal arrangement of the adsorbate. For hexagonal substrate lattices the simulation demonstrates that various adsorbate structures (from honeycomb lattices to quasicrystalline pentagonal configurations) may be observed, depending on the effective radii of interaction. Due to the long-ranged coupling the substrate may acquire a substructure induced by the adsorbate. This paper represents a generalization of the work published in *Phys. Rev. Lett.* **81**, 3904 (1998). [S1063-651X(99)01107-1]

PACS number(s): 68.45.-v

I. INTRODUCTION

Theoretical treatments of solid-liquid interfaces are traditionally based on the assumption that the solid side remains unchanged under the influence of the adsorbate, while the latter is adjusted to a potential relief of the solid substrate [1,2]. This approximation is justified in most cases when an interaction between the substrate particles is much stronger than that between the adsorbates [3]. The ordering [4] and interfacial rearrangement of adsorbates are mainly determined by the symmetry of the substrate. Various orientationally ordered structures may appear under the influence of the substrate-induced strain [5].

Another situation takes place when the surface has some latent instability due to the termination of the bulk crystalline structure. Then the positions of the ideal termination do not correspond to a minimum of the surface free energy and the surface atoms tend to a new arrangement [6]. This is observed for {100} and {110} surfaces of transition metals which may reconstruct upon cooling or due to adsorption [7]. The latter case represents the so-called adsorbate-induced reconstruction. The role of an adsorbate is to reduce the surface tension and, therefore, to stabilize one of the possible lattice configurations provided by the substrate. A typical example is the hydrogen-induced reconstruction of W{001}, when the adsorption causes the substrate to prefer one of four equally available configurations [7,8].

For realistic unreconstructed interfaces the adsorbate-induced effects are not negligible. A surface may exhibit stability or instability with respect to adsorption depending on the nature of the adsorbate. This is due to the fact that the adsorbate-substrate bonding energy can be comparable to, or

even larger than, the cohesive energy of the substrate [9]. It is demonstrated [10] that adsorption may lead to significant lowering of the roughening temperature. Adsorption isotherms for surfaces with dynamically changing morphology exhibit nontrivial changes compared to the rigid substrate case [11]. Restructuring of metal surfaces under the adsorbate-induced stress [12] is also well detected [13–15]. These experiments have suggested that the stress is due to the charge redistribution at the interface. The surface stress contributes significantly to the elastic energy and can give rise to a self-organization of mesoscopic structures at the interface. Recent experimental investigations [16] of adsorption at close packed surfaces have suggested that some local distortion of Au{111} surfaces should be assumed in order to interpret the diffraction patterns of *n*-alkyl thiols. Similar buckling and lateral shifts are detected [17] for Ru{001} in the presence of adsorbed oxygen.

In our previous studies [18,19] we have suggested a mechanism for the distortion of dynamically changing substrates affected by an adsorbate with strong lateral interactions. The latter tends to stabilize the hexagonal arrangement of the overlayer (with increasing density or decreasing temperature). The adsorbent-adsorbate interaction favors an arrangement compatible with the substrate symmetry. In the presence of a strong pinning of the adsorbate and the substrate displacive degrees of freedom, one may expect a distortive rearrangement in the substrate [18] or even melting of the substrate supplemented by a fragmentation of the adsorbate [19]. In this paper we present a more complete theoretical account of this mechanism as well as Brownian dynamics (BD) results which demonstrate that various structures may result from the competing interactions at the interface. We consider the solid-liquid interface, that is, the coverage depends on the thermodynamic conditions in the bulk liquid as well as on the displacements of the adsorbent. Therefore, the adsorbate is not presumably ordered as in the case of thin films. It should be noted that we do not specify any concrete system for which experimental information is available. Nevertheless our theoretical analysis is applicable to a broad

*Permanent address: Institute for Condensed Matter Physics, Svientsitsky strasse 1, 290011, Lviv, Ukraine.

†Permanent address: Donetsk Physical-Technical Institute of NASU, 340114 Donetsk, Ukraine.

‡Author to whom correspondence should be addressed.

class of interfaces where all the interactions are of the same order of magnitude. Of course, the next step should be taken towards quantitative comparison of our results with experiments.

The paper is organized as follows. In Sec. II we specify the analytical model. Then in Sec. III we calculate the free energy in the mean-field approximation and determine the order parameter. The results of the BD simulation are presented in Sec. IV. Section V contains our conclusion.

II. THE MODEL

We consider a liquid in contact with an adsorbing crystalline substrate. The substrate is assumed to be stable, that is, without the adsorbate it keeps a given crystalline configuration up to the melting temperature. The surface of the substrate is represented by a square two-dimensional array of atoms. Each atom holds an adsorbing site able to attract the molecules of the liquid. The total number of the sites is N_s and S is the surface area. The lattice spacing and the effective diameter of the liquid molecule are denoted as d and σ , respectively. The sites are assumed to have dispersive degrees of freedom which are due to the elastic properties (phononic excitations or anharmonicity effects) of the substrate. In the absence of the adsorbate these displacements represent the usual vibration of the solid atoms around the equilibrium positions $\{\mathbf{R}_i^0\}$, such that the average distortion $\langle \mathbf{u}_i \rangle = \mathbf{R}_i - \mathbf{R}_i^0$ is zero. The Hamiltonian is

$$H = H_S + H_L + H_{SL}, \quad (1)$$

where the contributions corresponding to the substrate and to the liquid are given by

$$H_S = \sum_{ij} U_{SS}(\mathbf{R}_i, \mathbf{R}_j), \quad H_L = \sum_{\alpha, \beta} U_{LL}(\mathbf{r}_\alpha, \mathbf{r}_\beta). \quad (2)$$

Here \mathbf{R}_i and \mathbf{r}_α denote the positions of the substrate and the liquid particles, respectively. For the sake of simplicity we assume that the motion of the substrate units in the direction perpendicular to the surface is forbidden. Thus, the vectors corresponding to the solid part are two dimensional. The pair potentials for the solid and for the liquid are given by the values of U_{SS} and U_{LL} . Note that the H_S does not describe the entire substrate side but only the part involved in the coupling with the liquid. The liquid is confined to a half space limited by the plane. The coupling term is defined to be the sum of pair potentials:

$$H_{SL} = \sum_{i, \alpha} U_{SL}(\mathbf{R}_i, \mathbf{r}_\alpha). \quad (3)$$

The Boltzmann factor formed by this potential can be written in terms of the Mayer functions $f_{SL}(\mathbf{R}_i, \mathbf{r}_\alpha)$ as

$$\begin{aligned} & \exp \left\{ -\beta \sum_{i, \alpha} U_{SL}(\mathbf{R}_i, \mathbf{r}_\alpha) \right\} \\ &= \prod_{i, \alpha} \{ 1 + f_{SL}(\mathbf{R}_i, \mathbf{r}_\alpha) \} \\ &= \prod_{\alpha} \left\{ 1 + \sum_i f_{SL}(\mathbf{R}_i, \mathbf{r}_\alpha) \right. \\ & \quad \left. + \frac{1}{2!} \sum_{ij} f_{SL}(\mathbf{R}_i, \mathbf{r}_\alpha) f_{SL}(\mathbf{R}_j, \mathbf{r}_\alpha) + \dots \right\}. \quad (4) \end{aligned}$$

We consider strongly attractive and saturable forces, so that we can assume that a given molecule of the liquid occupies a single site at the surface. The site is then ‘‘disabled’’ for further adsorption. In this case we have

$$\exp \left\{ -\beta \sum_{i, \alpha} U_{SL}(\mathbf{R}_i, \mathbf{r}_\alpha) \right\} = \prod_{\alpha} \left\{ 1 + \sum_i f_{SL}(\mathbf{R}_i, \mathbf{r}_\alpha) \right\}. \quad (5)$$

The Mayer function is chosen to be that of the sticky potential [20–23]:

$$f_{SL}(\mathbf{R}_i, \mathbf{r}_\alpha) = \lambda \delta(\mathbf{R}_i - \mathbf{R}_\alpha) \delta(z_\alpha - \sigma/2), \quad (6)$$

where \mathbf{R}_α is the plane projection of \mathbf{r}_α , λ is the stickiness parameter, $\beta = 1/kT$, and z_α is the distance to the wall. This potential states that a molecule can be adsorbed at the lattice if its current position coincides with the position of a lattice site.

Note that such a procedure is valid for a description of the chemisorption processes, but for the physisorbed systems (like the noble gases on graphite) the contributions from all lattice sites should be taken into account to give a proper gas-solid potential [3]. It should be noted also that we associate a site with a substrate atom. This implicitly means that we consider the on-top sites only. In order to account for other types (bridge or hollow) of adsorbing sites, it is necessary to introduce a relation between the displacement of a site and the displacement of a group of solid atoms.

III. FREE ENERGY

The partition function of our problem is

$$\begin{aligned} Z &= \frac{1}{C_S} \int (d\mathbf{R}_i) e^{-\beta H_S} \frac{1}{C_L} \int (d\mathbf{r}_\alpha) e^{-\beta H_L} \\ & \quad \times \prod_{\alpha} \left\{ 1 + \lambda \sum_i \delta(\mathbf{R}_i - \mathbf{R}_\alpha) \delta(z_\alpha - \sigma/2) \right\}. \quad (7) \end{aligned}$$

Here C_L and C_S are the normalization constants, $(dA_i) = \prod_{i=1}^{N_k} dA_i$, with N_k being the total number of molecules of type k . Integration over the liquid positions gives the result [20–23]

$$Z = Z_L^0 \frac{1}{S^{N_s}} \int (d\mathbf{R}_i) e^{-\beta \sum_{i,j} U_{SS}(\mathbf{R}_i, \mathbf{R}_j)} \times \sum_{n=0}^{N_s} \frac{\lambda^n}{n!} \sum_{\mathbf{R}_n} \rho_n^0(\mathbf{R}_1, \dots, \mathbf{R}_n). \quad (8)$$

Here Z_L^0 is the partition function of the liquid near the hard wall (i.e., without the coupling), $\rho_n^0(\mathbf{R}_1, \dots, \mathbf{R}_n)$ is the n -body distribution function for the same system, taken at the lattice positions. The result above is quite similar to that obtained in Refs. [20–23] for lattices with fixed sites. The only difference is that we have an additional integration over the lattice positions. Therefore, we express the $\rho_n^0(\mathbf{R}_1, \dots, \mathbf{R}_n)$ through the n -body correlation function $g_n^0(\mathbf{R}_1, \dots, \mathbf{R}_n)$,

$$\rho_n^0(\mathbf{R}_1, \dots, \mathbf{R}_n) = g_n^0(\mathbf{R}_1, \dots, \mathbf{R}_n) \prod_{i=1}^n \rho_1^0(\sigma/2)$$

and use the Kirkwood superposition approximation:

$$g_n^0(\mathbf{R}_1, \dots, \mathbf{R}_n) = \prod_{i,j=1}^n g_2^0(\mathbf{R}_i, \mathbf{R}_j).$$

After these rearrangements the partition function takes the form

$$\Xi = \frac{Z}{Z_L^0} = \frac{1}{S^{N_s}} \int (d\mathbf{R}_i) e^{-\beta \sum_{i,j} U_{SS}(\mathbf{R}_i, \mathbf{R}_j)} \times \sum_{n=0}^{N_s} \frac{(\lambda \rho_1^0)^n}{n!} e^{-\beta \sum_{i,j} W_{LL}(\mathbf{R}_i, \mathbf{R}_j)}, \quad (9)$$

where we have introduced the mean force potential for the liquid

$$-\beta W_{LL}(\mathbf{R}_i, \mathbf{R}_j) = \ln g_2^0(\mathbf{R}_i, \mathbf{R}_j). \quad (10)$$

Notice that the summation over i, j for the mean force potential is restricted to $i, j = 1, n$. In order to avoid this inconvenience we introduce the occupation numbers t_i [20–23],

$$\Xi = \frac{1}{S^{N_s}} \int (d\mathbf{R}_i) e^{-\beta \sum_{i,j} U_{SS}(\mathbf{R}_i, \mathbf{R}_j)} \times \sum_{t_i} e^{-\beta \sum_{i,j} W_{LL}(\mathbf{R}_i, \mathbf{R}_j) t_i t_j} e^{\beta \sum_i \mu_i t_i} \quad (11)$$

where the quantity

$$\beta \mu_i = \ln[\lambda \rho_1^0(\sigma/2)] \quad (12)$$

plays the role of the chemical potential for the adsorbate. In fact, each pair of the solid sites interacts through U_{SS} potential plus an extra W_{LL} contribution, if these sites have a pair of adsorbed molecules. The presence of this additional interaction is determined by the set of occupation numbers. The partition function (11) describes a coupling of a translationally invariant system (the substrate) with the adsorbate which is not translationally invariant (at least on the same scale).

Even an ordered $\{m \times n\}$ overlayer differs in the periodicity and the symmetry from the underlying lattice. In our case the adsorbate is not presumably ordered. Only at very high densities will the spherically symmetric W_{LL} interaction favor a solidlike hexagonal arrangement. Similar coupling between the “spin” and elastic degrees of freedom was studied [24–26] in context of magnetoelasticity effects. Nevertheless, the main focus of the above studies was on the influence of an elastic subsystem on the criticality of the Ising one. We discuss a “reverse” problem—an elastic subsystem (the substrate) under the influence of the Ising-like counterpart (the adsorbate). In order to reduce our problem to that of a pure solid with an effective Hamiltonian we should perform the summation over all possible configurations $\{t_i\}$ of adsorbed particles. We assume that $W_{LL}(\mathbf{R}_i, \mathbf{R}_j)$ does not change the sign at distances of order of the lattice spacing d , so that we avoid frustration effects [27]. Then the summation over the occupation numbers can be performed within the usual mean-field approximation (MFA) [1,18],

$$W_{LL}(\mathbf{R}_i, \mathbf{R}_j) t_i t_j \approx W_{LL}(\mathbf{R}_i, \mathbf{R}_j) \langle t_i \rangle t_j + W_{LL}(\mathbf{R}_i, \mathbf{R}_j) t_i \langle t_j \rangle - W_{LL}(\mathbf{R}_i, \mathbf{R}_j) \langle t_i \rangle \langle t_j \rangle$$

to give the result

$$\Xi = \frac{1}{S^{N_s}} \int (d\mathbf{R}_i) e^{-\beta/2 \sum_{i,j} U_{SS}(\mathbf{R}_i, \mathbf{R}_j)} \times e^{\beta/2 \sum_{i,j} W_{LL}(\mathbf{R}_i, \mathbf{R}_j) \Theta_i \Theta_j} \times \prod_i [1 + e^{\beta(\mu_i - \sum_j W_{LL}(\mathbf{R}_i, \mathbf{R}_j) \Theta_j)}], \quad (13)$$

where $\Theta_i = \langle t_i \rangle$ is the average occupation number at the site numbered i . This quantity should be determined self-consistently by the minimization of the free energy. The factor 1/2 is introduced in order to avoid double counting.

To proceed further we extract the contribution corresponding to the reference state, i.e., the state with the sites located at the equilibrium positions.

$$U_{SS}(\mathbf{R}_i, \mathbf{R}_j) = U_{SS}(\mathbf{R}_i^0, \mathbf{R}_j^0) + U_{SS}(\mathbf{u}_i, \mathbf{u}_j),$$

$$W_{LL}(\mathbf{R}_i, \mathbf{R}_j) = W_{LL}(\mathbf{R}_i^0, \mathbf{R}_j^0) + W_{LL}(\mathbf{u}_i, \mathbf{u}_j),$$

where $\mathbf{u}_i = \mathbf{R}_i - \mathbf{R}_i^0$ is the displacement vector. The partition function can be reduced to the form

$$\Xi = e^{-\beta F_0(\Theta)} \int (d\mathbf{u}_i) e^{-\beta/2 \sum_{i,j} U_{SS}(\mathbf{u}_i, \mathbf{u}_j)} \times e^{\beta/2 \sum_{i,j} W_{LL}(\mathbf{u}_i, \mathbf{u}_j) \Theta_i \Theta_j} \prod_i [1 + \tau_i(\Theta)] \times \{e^{-\beta \sum_j W_{LL}(\mathbf{u}_i, \mathbf{u}_j) \Theta_j} - 1\}, \quad (14)$$

where $F_0(\Theta)$ and $\tau_i(\Theta)$ are given by

$$F_0(\Theta) = -\frac{1}{2} \sum_{ij} W_{LL}(\mathbf{R}_i^0, \mathbf{R}_j^0) \Theta_i \Theta_j + \frac{1}{\beta} \sum_i \ln\{1 - \tau_i(\Theta)\}, \quad (15)$$

$$\tau_i(\Theta) = \frac{e^{\beta\mu_i - \beta\Sigma_j W_{LL}(\mathbf{R}_i^0, \mathbf{R}_j^0)\Theta_j}}{1 + e^{\beta\mu_i - \beta\Sigma_j W_{LL}(\mathbf{R}_i^0, \mathbf{R}_j^0)\Theta_j}}. \quad (16)$$

In the absence of the displacement part the equations above describe the free energy and adsorption isotherm for the rigid substrate [$\Theta_i = \tau_i(\Theta)$]. In general, $F_0(\Theta)$ and $\tau_i(\Theta)$ are just convenient notations, since the coverage should be calculated from the free energy which is determined from Eq. (14).

A. Harmonic approximation

The displacement dependent contributions to the potentials may be represented by their Taylor expansions around the equilibrium positions.

$$U_{SS}(\mathbf{u}_i, \mathbf{u}_j) = V_S(\mathbf{u}_i) + D_{ij}\mathbf{u}_i \cdot \mathbf{u}_j + \dots, \quad (17)$$

$$W_{LL}(\mathbf{u}_i, \mathbf{u}_j) = V_L(\mathbf{u}_i) + \Delta_{ij}\mathbf{u}_i \cdot \mathbf{u}_j + \dots, \quad (18)$$

where D_{ij} and Δ_{ij} are the elastic matrices given by

$$D_{ij} = \left[\frac{\partial^2 U_{SS}(\mathbf{R}_i, \mathbf{R}_j)}{\partial \mathbf{R}_i \partial \mathbf{R}_j} \right]_{\mathbf{R}_i^0, \mathbf{R}_j^0}, \quad \Delta_{ij} = \left[\frac{\partial^2 W_{LL}(\mathbf{R}_i, \mathbf{R}_j)}{\partial \mathbf{R}_i \partial \mathbf{R}_j} \right]_{\mathbf{R}_i^0, \mathbf{R}_j^0}. \quad (19)$$

Expansion (18) may contain a linear term which is dropped assuming that the equilibrium positions of the substrate lattice are close to extrema of $W_{LL}(\mathbf{u}_i, \mathbf{u}_j)$. For the substrate lattice such a representation is quite natural because of the symmetry arguments [28]. For the liquid the mean force potential is an oscillating function, exponentially decaying within a correlation length. Thus, the small displacement series may seem questionable in this case. But actually, we are interested in the liquid behavior in the neighborhood of the equilibrium positions of the lattice. If the long-range effects are not prominent, then we may use the expansion above.

The one-particle potentials are

$$V_S(\mathbf{u}_i) = V_S^0(\mathbf{u}_i) + \sum_j \left[\frac{\partial^2 U_{SS}(\mathbf{R}_i, \mathbf{R}_j)}{\partial \mathbf{R}_i \partial \mathbf{R}_i} \right]_{\mathbf{R}_i^0, \mathbf{R}_j^0} \mathbf{u}_i^2 = a_i \mathbf{u}_i^2, \quad (20)$$

$$V_L(\mathbf{u}_i) = \sum_j \left[\frac{\partial^2 W_{LL}(\mathbf{R}_i, \mathbf{R}_j)}{\partial \mathbf{R}_i \partial \mathbf{R}_i} \right]_{\mathbf{R}_i^0, \mathbf{R}_j^0} \mathbf{u}_i^2 = \alpha_i \mathbf{u}_i^2, \quad (21)$$

where $V_S^0(\mathbf{u}_i)$ is the substrate potential in the absence of the displacement correlations at the surface. In fact, this contribution represents an impact from the solid bulk. In general, the expansions given above may contain higher-order terms, which account for a nonparabolicity of the one-particle potentials and the many-body interaction among the displacements. For the case of small displacements we can restrict ourselves by the harmonic approximation. It is worth noting that the force constants a_i and D_{ij} are positively defined due to the thermodynamical stability of the solid side. In contrast, the values of α_i and Δ_{ij} are determined by the properties of the liquid within the range of distances comparable with the lattice spacing d . This means that the latter quantities may be

positive or negative depending on the nature of the liquid and the thermodynamical conditions for the adsorption.

For instance, if the $W_{LL}(R)$ is the hard sphere mean force potential, then the curvature at $R = 3\sigma/2$ is negative, its magnitude increases with increasing density. If $d = 3\sigma/2$ then a pair of adsorbed molecules will tend to reduce [$W(\mathbf{R}_i^0, \mathbf{R}_j^0) < 0$] or to extend [$W(\mathbf{R}_i^0, \mathbf{R}_j^0) > 0$] the separation. Therefore, a negative curvature may take place when the adsorbate size differs from that of the substrate. For systems with specific interactions the curvature is temperature dependent.

Within the harmonic approximation for the potentials the partition function takes the form

$$\Xi = e^{-\beta F_0(\Theta)} \int (d\mathbf{u}_i) e^{-\beta/2\Sigma_i a_i \mathbf{u}_i^2} \times e^{-\beta/2\Sigma_{i,j} D_{ij} \mathbf{u}_i \cdot \mathbf{u}_j} e^{-\beta U_{SL}(\mathbf{u}_i, \mathbf{u}_j)}, \quad (22)$$

where the displacement-dependent contribution $U_{SL}(\mathbf{u}_i, \mathbf{u}_j)$ is given by

$$U_{SL} = -\frac{1}{2} \sum_i \alpha_i \mathbf{u}_i^2 \Theta_i^2 - \frac{1}{2} \sum_{ij} \Delta_{ij} \mathbf{u}_i \cdot \mathbf{u}_j \Theta_i \Theta_j - \frac{1}{\beta} \sum_i \ln[1 + \tau_i(\Theta) \{e^{-\beta\alpha_i \mathbf{u}_i^2 \Theta_i} \times e^{-\beta\Sigma_j \Delta_{ij} \mathbf{u}_i \cdot \mathbf{u}_j \Theta_j} - 1\}]. \quad (23)$$

The logarithmic term results from the product in Eq. (14). Thus we see that, despite the harmonic approximation used, the displacement contribution of the liquid part is not harmonic. This is due to the fact that the mean force potential is not applied to all the surface sites simultaneously, but only to the adsorbed positions. One may expect some unbalanced forces at the domain walls between the covered and uncovered parts of the surface. These forces result in the anharmonicity and the many-body interaction given by the logarithmic term which originates from the entropy associated with different adsorbate configurations at fixed coverage. For low coverages the concentration of the domain walls vanishes and the logarithm and the exponential could be linearized. Then the liquid contribution is harmonic,

$$U_{SL} = \sum_i \alpha_i T_{ii}(\Theta) \mathbf{u}_i^2 + \sum_{ij} \Delta_{ij} T_{ij}(\Theta) \mathbf{u}_i \cdot \mathbf{u}_j, \quad (24)$$

where $T_{ij}(\Theta)$ is given by

$$T_{ij}(\Theta) = \tau_i(\Theta) \Theta_j - \frac{1}{2} \Theta_i \Theta_j. \quad (25)$$

At this level we have an effective harmonic Hamiltonian with the dynamic matrix renormalized by the overlayer effects. For arbitrary coverages the potential should be taken as it stands. Therefore, the complicated form of the U_{SL} is the price we have to pay for the transformation of the random adsorbate configurations into a translationally invariant potential. In order to estimate possible effects of this potential we first analyze the one-body term

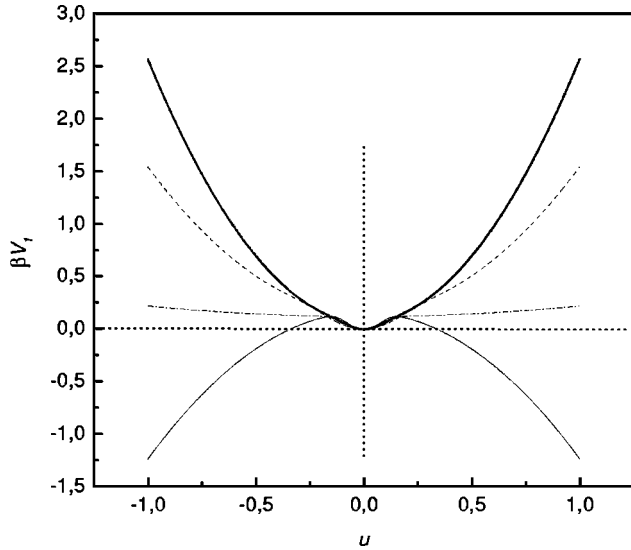


FIG. 1. The one-particle potential βV_1 (harmonic approximation) as a function of the dimensionless displacement u . The curves correspond to $\alpha/a=0$ (bold solid); $\alpha/a=2, \Theta=0.5$ (dashed); $\alpha/a=-2, \Theta=0.2$ (dashed-dotted); $\alpha/a=-2, \Theta=0.4$ (solid). All the quantities are dimensionless (see text).

$$V_1 = \sum_i v(\mathbf{u}_i) = \frac{1}{2} \sum_i a_i \mathbf{u}_i^2 - \frac{1}{2} \sum_i \alpha_i \mathbf{u}_i^2 \Theta_i^2 - \frac{1}{\beta} \sum_i \ln[1 + \tau_i(\Theta) \{e^{-\beta \alpha_i \mathbf{u}_i^2 \Theta_i} - 1\}]. \quad (26)$$

In Fig. 1 the value of βV_1 is plotted as a function of the dimensionless displacement variable $u = u_i/d$. It is seen that the potential becomes flatter with increasing coverage. This takes place for positive and for negative α_i . The equilibrium position $u=0$ is unstable if we allow for a large Θ . This suggests that the adsorbate causes a random hardening ($\alpha_i > 0$) or softening ($\alpha_i < 0$) of the substrate. The latter loses stability when the fraction of distorted bonds achieves a certain value. A rough estimation of this fraction using the linearization of Eq. (26) shows that the adsorbate part of the potential is negative at $1 - 2\Theta\tau(\Theta) > 0$ for positive α_i and $1 - 2\Theta\tau(\Theta) < 0$ for negative α_i . Under the condition $\tau(\Theta) \rightarrow 1$ we have a peculiarity for $\Theta \approx 1/2$, which is consistent with our previous estimation [19].

This instability does not mean a limitation imposed on Θ , since the coverage is proportional to the stickiness parameter λ , which may be chosen arbitrary (at least, within the model). The instability results from the harmonic approximation applied to the substrate. It is qualitatively similar to the harmonic instability of the regular lattices [29]. The principal difference of our case is that a new set of the equilibrium positions is not totally controlled by the symmetry of the lattice. In fact, we have a competition between the square lattice of the substrate and the hexagonal arrangement to which the adsorbate tends. To realize the meaning of this effect we have to include the anharmonicity of the substrate and the correlation between the displacements.

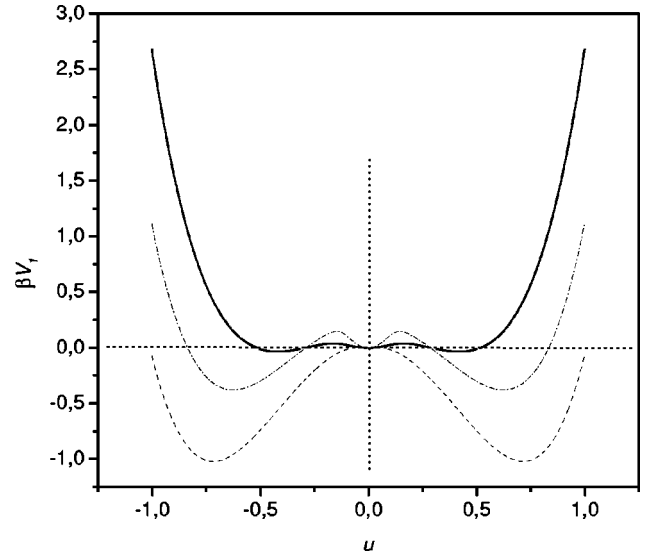


FIG. 2. The one-particle potential βV_1 (anharmonic approximation, $\gamma_i = 1 \times 10^{-3}$) as a function of the dimensionless displacement u . The curves correspond to $\alpha/a=-2, \Theta=0.4$ (bold solid); $\alpha/a=2, \Theta=0.7$ (dashed-dotted); $\alpha/a=-2, \Theta=0.7$ (dashed). All the quantities are dimensionless (see text).

B. Anharmonic effects and displacement correlation

There are two possible sources of anharmonic effects. These may come from the substrate side and/or from the adsorbate. The latter case reflects the existence of the preferential positions for the coverage. Actually these two factors are in competition, since they are favored by the potentials of different symmetries. In this paper we choose the simplest way and take into account only the substrate anharmonicity. The effective one-body potential of the adsorbate is already anharmonic, but not at the level of the bare potential W_{LL} . Despite some limitations, this approach suffices for our purposes.

Suppose that the substrate one-particle potential contains a fourth-order term, such that the resulting potential is

$$V_1 = \frac{1}{2} \sum_i a_i \mathbf{u}_i^2 - \frac{1}{2} \sum_i \alpha_i \mathbf{u}_i^2 \Theta_i^2 + \sum_i \gamma_i \mathbf{u}_i^4 - \frac{1}{\beta} \sum_i \ln[1 + \tau_i(\Theta) \{e^{-\beta \alpha_i \mathbf{u}_i^2 \Theta_i} - 1\}]. \quad (27)$$

The logarithmic term is conserved in the form found in the preceding section. The coefficient γ_i is positive, thus, the substrate potential is single wellled. As is shown in Fig. 2, the adsorbate term transforms βV_1 into a double- or even triple-welled potential. Had we included the anharmonicity of the adsorbate potential, we would observe multiple wells. This suggests that the adsorbate drives the substrate to a set of new equilibrium positions. The number of new positions and their location inside the initial unit cell depend on the nature of the adsorbate (the sign and the magnitude of α_i) and also on the coverage. Note that in the triple-welled case the substrate equilibrium position remains accessible (although, less stable), but in the double-welled case it is unstable. In the absence of the correlation between the cells, the substrate is driven to a disordered configuration, since there is no pref-

erence between the minima (at least between the deepest ones). Taking the correlations into account, we may expect some ordering. Different tools are appropriate for this aim. Depending on the geometry of the double-welled potential, the limiting cases of the displacive or the order-disorder instabilities may be distinguished [30,31]. In the case of two deep minima separated by a high barrier the problem can be treated within the pseudospin formalism [29], while for a low barrier potential the soft mode concept is more appropriate. This allows us to predict which of two positions is actually realized in the presence of the correlation.

Unfortunately, it is difficult to apply these methods to our problem, because the one-particle potential changes with the coverage. The latter should be determined self-consistently from the free energy calculated with this potential. For this reason we restrict ourselves by a range of the parameters at which the potential keeps the triple-welled shape (the bold curve in Fig. 2). If the barriers between the minima are low, we can approximate this potential by the square well.

$$V_1 = \begin{cases} -U_0, & |\mathbf{u}_i| < L/2 \\ \infty & \text{otherwise,} \end{cases} \quad (28)$$

where U_0 is the depth of the well and L is its width. The cutoff distance L corresponds to the flat bottom region of the real anharmonic potential. In addition to the one-body potential we consider the bilinear correlation term. It contains the substrate contribution $\sum_{ij} D_{ij} \mathbf{u}_i \mathbf{u}_j$ and the bilinear combination $\sum_{ij} T_{ij}(\Theta) \Delta_{ij} \mathbf{u}_i \mathbf{u}_j$, extracted from the U_{SL} . Now the $T_{ij}(\Theta)$ function has a more complicated form which reduces to Eq. (25) in the limit of low coverages. For simplicity we assume the uniaxial anisotropy [31] along a virtual external field v_i .

$$\mathbf{u}_i \cdot \mathbf{u}_j = u_i u_j \cos(\varphi_{ij}) = \begin{cases} u_i u_j, & \varphi_{ij} = 0 \\ -u_i u_j, & \varphi_{ij} = \pm \pi \end{cases} \quad (29)$$

where φ_{ij} is the angle between two displacement vectors. Therefore each u_i is a scalar confined between $-L/2$ and $L/2$. Then our problem becomes quasi-one-dimensional, with the partition function given by

$$\Xi = e^{-\beta F_0(\Theta)} e^{\beta U_0} \frac{1}{L} \int_{-L/2}^{L/2} (du_i) \times e^{-\beta \sum_{i,j} [D_{ij} + T_{ij}(\Theta) \Delta_{ij}] u_i u_j} e^{-\beta \sum_i v_i u_i}, \quad (30)$$

where v_i is a virtual displacement field introduced for convenience in further calculations. Introducing the MFA for the displacements, we get the free energy excess

$$\beta F = \beta F_0(\Theta) - \beta U_0 - \frac{1}{2} \sum_{i,j} [D_{ij} + T_{ij}(\Theta) \Delta_{ij}] \langle u_i \rangle \langle u_j \rangle - \sum_i \ln I[\langle u_i \rangle], \quad (31)$$

where

$$I[\langle u_i \rangle] = \frac{\sinh \left\{ v_i + \sum_j [D_{ij} + T_{ij}(\Theta) \Delta_{ij}] \langle u_j \rangle \right\}}{\left\{ v_i + \sum_j [D_{ij} + T_{ij}(\Theta) \Delta_{ij}] \langle u_j \rangle \right\}}. \quad (32)$$

Here we introduced the dimensionless quantities

$$v_i \rightarrow \beta v_i \frac{L}{2}, \quad \langle u_i \rangle \rightarrow \langle u_i \rangle \frac{1}{L}, \quad D_{ij} \rightarrow \beta D_{ij} \left(\frac{L}{2} \right)^2, \\ \Delta_{ij} \rightarrow \beta \Delta_{ij} \left(\frac{L}{2} \right)^2.$$

Minimization of the free energy with respect to the average displacements $\langle u_i \rangle$ gives the following self-consistent relation:

$$\langle u_i \rangle = -\mathcal{L} \left[v_i + \sum_j [D_{ij} + T_{ij}(\Theta) \Delta_{ij}] \langle u_j \rangle \right], \quad (33)$$

where $\mathcal{L}(x) = \coth(x) - 1/x$ is the Langevin function. It is easy to verify that Eq. (33) agrees with the definition of $\langle u_i \rangle$,

$$\langle u_i \rangle = - \left. \frac{\partial \beta F}{\partial v_i} \right|_{v_i=0}. \quad (34)$$

The second derivative gives the displacement correlation function

$$\chi_{ij} = - \left. \frac{\partial^2 \beta F}{\partial v_i \partial v_j} \right|_{v_i=0} = \frac{\partial \langle u_i \rangle}{\partial v_j} = \langle u_i u_j \rangle - \langle u_i \rangle \langle u_j \rangle. \quad (35)$$

In general, Eq. (33) may have many solutions depending on how many different interaction terms (D_{ij} and Δ_{ij}) are taken into account. For the simplest case of the nearest neighbor (NN) approximation we have

$$\langle u \rangle = -\mathcal{L}[q(D + T(\Theta)\Delta)\langle u \rangle], \quad (36)$$

$$\chi = \langle u^2 \rangle - \langle u \rangle^2 = \frac{S[q(D + T(\Theta)\Delta)\langle u \rangle]}{1 - q(D + T(\Theta)\Delta)S[q(D + T(\Theta)\Delta)\langle u \rangle]}, \quad (37)$$

where $S[x] = 1/x^2 - 1/\sinh^2(x)$ and q is the coordination number of the lattice. The virtual field v is turned off. Equation (36) has a nontrivial solution under the condition

$$q(D + T(\Theta)\Delta) \leq -3. \quad (38)$$

This equation represents an interplay between the elastic energies of the adsorbate and the substrate. For the substrate D is positively defined because of the thermodynamical stability, while Δ is negative for repulsive (NN) interactions. This indicates that the set of $\{\mathbf{R}_i^0\}$ is close to the maxima of W_{LL} . Then the adsorbate tends to shift from $\{\mathbf{R}_i^0\}$ to minimize the energy. If the coupling is strong, then the substrate is also involved in this motion. We deal with a distortive transition from the substrate-induced ordering ($\langle u_i \rangle = 0$) to that induced by the adsorbate ($\langle u_i \rangle \neq 0$). Within the square well approximation (28) this effect is described as a local

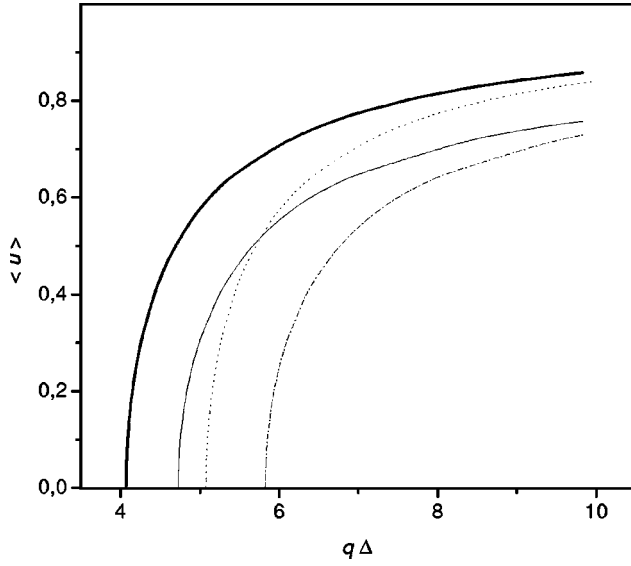


FIG. 3. The mean distortion $\langle u \rangle$ as a function of $q\Delta$. $D=1, \Theta=1$ (bold solid); $D=2, \Theta=1$ (dashed); $D=1, \Theta=0.9$ (solid); $D=2, \Theta=0.9$ (dashed-dotted). All the quantities are dimensionless (see text).

‘‘polarization’’ of the adsorbate sites due to the quasi-elastic energy induced by the adsorbate. The threshold (38) is Θ dependent, so that for a given Δ there exists some threshold coverage which should be determined self-consistently. Minimizing the free energy with respect to the coverage Θ we get the following equation for the adsorption isotherm:

$$\Theta - \tau(\Theta) = - \frac{E_d W}{E_d + W} \Theta \tau(\Theta) [1 - \tau(\Theta)]. \quad (39)$$

where $E_d = (q/2)\Delta \langle u \rangle^2$ is the average distortion energy and $W = \beta q W_{LL}(d)$ is the interaction energy at the equilibrium positions. Equation (39) represents a difference of the coverages corresponding to the distorted (Θ) and undistorted [$\tau(\Theta)$] lattices. The difference is determined by an interplay between the distortion energy E_d and the equilibrium coupling W . If $E_d = 0$ we have $\Theta = \tau(\Theta)$, as it should be. Since E_d is negative for nonzero $\langle u \rangle$, the sign of $\Theta - \tau(\Theta)$ depends on the sign of W . Therefore, $\Theta > \tau(\Theta)$ for $W < 0$ and $\Theta < \tau(\Theta)$ for $W > 0$. This difference increases with increasing distortion energy. If the undistorted lattice is totally covered [$\tau(\Theta) \rightarrow 1$], then $\Theta = \tau(\Theta)$. This suggests that the strongest coupling is expected near $\tau(\Theta) \approx 1/2$. Note, however, that we are restricted by the Θ at which the square well approximation for the potential remains adequate. Therefore, the applicability of Eq. (39) is limited.

The average displacement is plotted in Fig. 3 as a function of Δ . It is seen as a shift of the threshold with increasing substrate rigidity D . The threshold signals the second-order phase transition between the substrate-induced (undistorted) phase and the adsorbate-induced (distorted) phase. The susceptibility χ diverges at the transition. The threshold is shifted to larger Δ with decreasing coverage. The asymptotic increase of $\langle u \rangle$ is slower for lower Θ . This fact agrees with the reduction of the distance between the shifted minima in Fig. 2.

IV. SIMULATION

To recover the structure appearing due to this transition, we perform the BD simulation [32] which allows us to go beyond the small distortions up to a complete rearrangement of the surface. A similar approach has been developed recently [33–38] in the framework of the generalized Frenkel-Kontorova model. We consider two interacting subsystems of $N_j \leq 1 \times 10^3$ particles (where $j=1,2$ for the substrate and for the adsorbate atoms, respectively). The case of $N_2/N_1 = 1$ is reported here. One of them is confined to the minima of the external periodic potential $V_0(\mathbf{R})$, which is used to model the square crystalline surface.

$$V_0(\mathbf{R}) = - \frac{B_0}{2\pi} \cos(2\pi \mathbf{R}_x) \cos(2\pi \mathbf{R}_y), \quad (40)$$

with the amplitude $B_0 = 1$ and the period $a = 1$.

In general, the substrate atoms can move from these minima being affected by the adsorbate. Another subsystem describes the adsorbate, which is attracted to the substrate (moving) atoms and does not interact with the (fixed) periodic potential directly. For simplicity we set both atomic masses $m_j = 1$. The equation of motion for the atomic coordinates \mathbf{R}_{ji} is

$$\ddot{\mathbf{R}}_{ji} + \eta \dot{\mathbf{R}}_{ji} + \frac{\partial}{\partial \mathbf{R}_{ji}} V_0(\mathbf{R}_{ji}) \delta_{j1} + \frac{\partial}{\partial \mathbf{R}_{ji}} \sum_{kl} V(\mathbf{R}_{ji} - \mathbf{R}_{kl}) = \delta F(\mathbf{R}_{ji}; t), \quad (41)$$

where $1 \leq i \leq N_j$. To model a thermal bath we apply the Gaussian random force $\delta F_{ji}(t)$,

$$\langle \delta F(\mathbf{R}_{ji}; t), \delta F(\mathbf{R}_{j'i'}; t') \rangle = 2\eta T \delta_{jj'} \delta(\mathbf{R}_{ji} - \mathbf{R}_{j'i'}) \delta(t - t'), \quad (42)$$

to all atoms. The coefficient $\eta = 1$ corresponds to the external viscous damping due to the energy exchange between the adsorbate and the substrate. It defines the system temperature T . We calculated the average square of velocity to control the temperature fixed $T = 1$. Note that some temperature limitation should be imposed. The temperature should not be too high. The thermal energy should be lower than the energy of interatomic interaction (otherwise the behavior would be the same as for a system of noninteracting atoms). On the other hand, it must be lower than the magnitude B_0 of the sinusoidal potential (otherwise the behavior would be the same as for a system without the external potential). The interaction potential is chosen to be

$$V(|\mathbf{R}_{jj'}|) = V_{jj'} \exp(-\mathbf{R}_{jj'}^2/a_{jj'}). \quad (43)$$

The interaction is repulsive within a subsystem ($V_{jj} > 0$) and is attractive for different subsystems ($V_{12} < 0$). To stabilize the system at short distances we introduce a short-range repulsing contribution $V_{21} > 0$ (where $V_{21} \ll V_{12}$ and $a_{21} \ll a_{12}$). The characteristic radii $a_{jj'}^{1/2}$ determine the range of the interaction. The potential magnitudes and radii are measured in terms of B_0 and a , respectively.

The results of numerical simulation are summarized in Figs. 4–7. In particular, Fig. 4(a) represents a small ($N \leq 2$

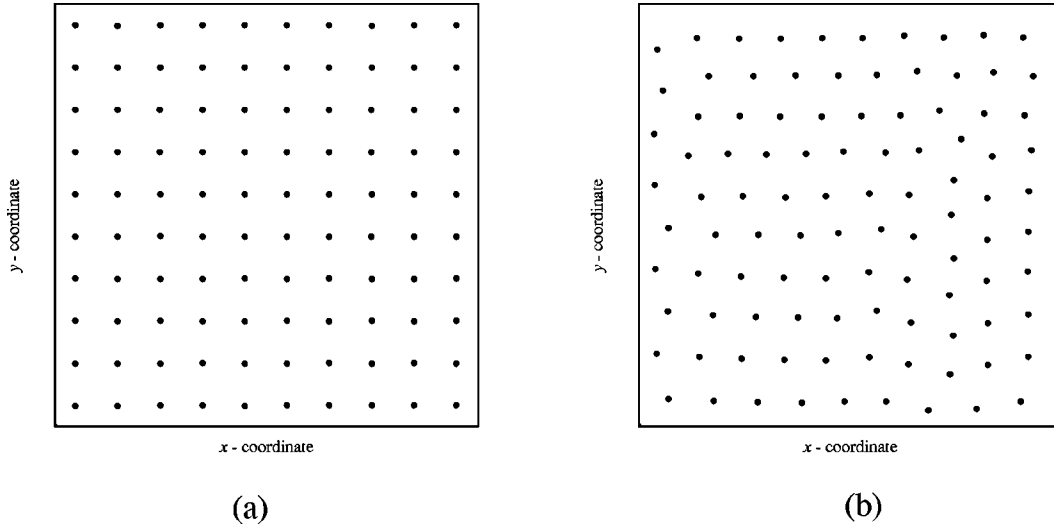


FIG. 4. Fragments of two characteristic initial and final substrate configurations: (a) initial ideal square lattice, (b) the adsorbate-driven structure corresponding to $V_{11}=V_{12}=50$, $V_{21}=V_{12}/2$, $V_{22}=3V_{12}$. Other model parameters were taken as follows: $a_{11}=a_{22}=0.875$, $a_{12}=0.5$, $a_{21}=0.0125$. All the quantities are dimensionless (see text).

$\times 10^2$ particles) fragment of the initial substrate configuration. This structure conserves if the interatomic interactions are negligible. At nonzero interaction the structure that develops in time usually consists of different symmetry domains [Fig. 4(b)]. Visually one can detect sixth-, fifth-, and fourth-order local axes. This makes the intermediate structures quite complicated for a quantitative description. The domain wall separating the substrate- and the adsorbate-driven structures is also well detected. Numerical solution of Eq. (41), supplemented by the periodic boundary conditions, enables us to calculate the density distributions $\varrho_j(\mathbf{R}) = \sum_i \delta(\mathbf{R} - \mathbf{R}_{ij})$ and, after the averaging, the two-body correlation functions $G_{j,j'}(\mathbf{R}, \mathbf{R}') = \langle \varrho_j(\mathbf{R}) \varrho_{j'}(\mathbf{R}') \rangle$ which are the quantitative measures of the configurations observed. The two-dimensional Fourier transform of the substrate correlation function

$$G_{11}(\mathbf{q}) = \int d(\mathbf{R} - \mathbf{R}') e^{i\mathbf{q}(\mathbf{R} - \mathbf{R}')} G_{11}(\mathbf{R}, \mathbf{R}') \quad (44)$$

represents our main focus. The distribution of its maxima is shown in Fig. 5. If the corrugation of B_0 dominates over the V_{12} and V_{22} , then both subsystems reach the square lattice structure, determined by the substrate [Fig. 5(b)]. If $V_{11} \ll V_{22}$, then the steady state has a distorted hexagonal symmetry [Fig. 5(a)].

Note that the ideal hexagonal structure may seem questionable since its symmetry group is not a subgroup of the square symmetry. On the other hand, the hexagonal symmetry is natural for the adsorbate, provided that the substrate is infinitely soft. Therefore, for a finite substrate rigidity we observe the distorted structure with two common reflection axes indicated. This makes a compromise between the square (unperturbed) structure and the hexagonal one driven by the adsorbate. All intermediate distributions appear as superpositions of these two limiting cases. Namely, the b, b' maxima (and complementary to them) disappear and the a, a' (and complementary) peaks grow if one passes from the substrate- to the adsorbate-driven structure. This is demonstrated in

Fig. 6, which represents the evolution of the specific peaks with increasing adsorbate-adsorbate interaction V_{22} .

The rate of interaction at which the b, b' peaks become indistinguishable is quite sensitive to the noise produced by the random force $\delta F_{ji}(t)$. In fact, these peaks do not disappear at all; they become comparable to the level of the noise.

According to the general approach [39], the normalized height difference of b (or b') peaks for two structures determines the order parameter which is depicted in Fig. 7. To estimate the time necessary to reach the steady state we set $V_{22} = V_{22}^{\max} = 50$ (this corresponds to the adsorbate-driven structure). All other parameters of the problem and the relations between them ($V_{11} = V_{12} = 50$, $V_{22} = 3V_{12}$, $V_{21}^0 = V_{12}^0/2$, $a_{11} = a_{22} = 0.875$, $a_{12} = 0.5$, $a_{21} = 0.0125$) are kept fixed. Here V_{ij} and a_{ij} are measured in terms of the corrugation amplitude B_0 and the initial lattice spacing, respectively. A typical example of such an estimation is presented in Fig. 7(a). Here we plot a time dependence of the order parameter. Two stages are clearly seen. At short times an intensive distortion of the square lattice takes place. After that the system slowly relaxes to the adsorbate-driven structure. The estimation gives $t_{\max} = 1.5 \times 10^2 \times \eta^{-1}$. The relative time is given in units of t_{\max} .

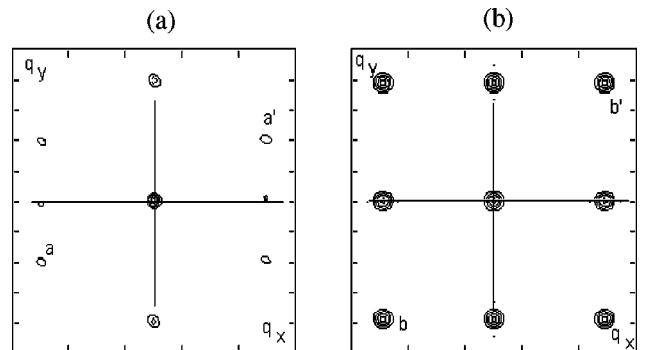


FIG. 5. Maxima of $G_{11}(\mathbf{q})$ for the substrate configurations shown in Fig. 4. The letters a, a' and b, b' denote the maxima specific for symmetrically different structures (see text). Dimensionless wave numbers are denoted as q_x and q_y .

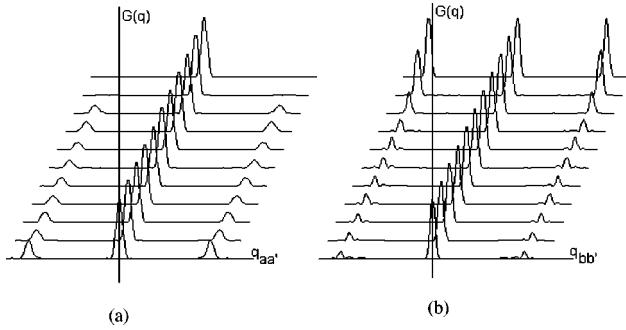


FIG. 6. Evolution of $G_{11}(\mathbf{q})$ with the change of V_{22} described in text. Other parameters are the same as in Fig. 4. Two sequences [(a) and (b), respectively] represent the transformations of the profiles along the directions aa' and bb' specified in Fig. 5. All the quantities are dimensionless (see text).

Then we increase the V_{22} from the trivial case of $V_{22} = 0$ up to V_{22}^{\max} . At each step we calculated the order parameter

$$P = 1 - G_{11}(\mathbf{q}_b; V_{22}) / G_{11}(\mathbf{q}_b; V_{22} = 0), \quad (45)$$

which is plotted in Fig. 7(b). The relative strength of interaction is determined as V_{22}/V_{22}^{\max} . Qualitatively the same result is observed when V_{12} changes at fixed V_{22} . Since the elastic matrices treated analytically are just the second derivatives of the potentials, the curvatures are proportional to the potential magnitudes. The proportionality coefficient disappears when the ratio is taken. This allows us to compare the theoretical prediction [from Eq. (36)] with the simulation result.

The asymptotic regime ($\langle u \rangle \rightarrow 1$), corresponding to the adsorbate-driven structure, is described correctly. But a deviation is seen near the threshold. This is due to the finite box size which leads to difficulties in extracting the b peak from the satellite fluctuations. The rate of interaction at which the b, b' peaks become indistinguishable is quite sensitive to the noise produced by the random force $\delta F_{ji}(t)$. Therefore the threshold should be associated with the inflection point [40] appearing at $V_{22}/V_{22}^{\max} \approx 0.154$ (the theory gives 0.183). The inflection point is clearly seen at Fig. 7(a). On the other hand, the threshold is predicted within the MFA, which is

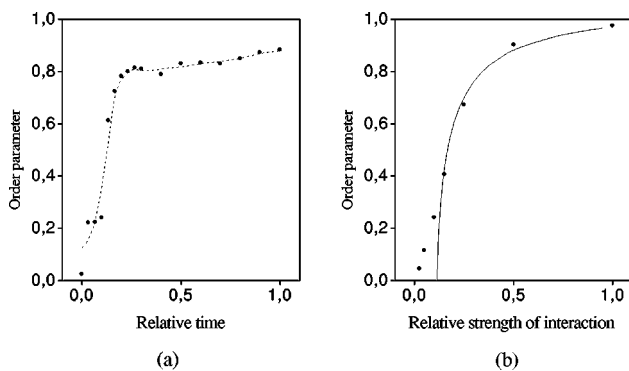


FIG. 7. The order parameter as a function of relative time and strength of interaction [(a) and (b), respectively]. Numerical results are shown by black circles. The dashed line in (a) gives a guide, the solid curve in (b) represents the analytical estimation obtained from Eq. (36).

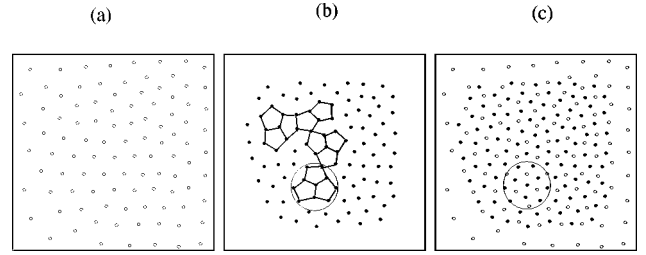


FIG. 8. Snapshots of the substrate (a), adsorbate (b), and common (c) structures. Encircled area shows typical arrangement of pentagons at the hexagonal substrate.

known [39] to be only qualitatively correct near the ordering transition. The latter cannot be qualified as the conventional commensurate-incommensurate transition [1], since both subsystems form a common lattice which, however, differs from that of the clean substrate. On the other hand, this is not the conventional reconstruction [6,7], because the substrate itself is stable. The instability towards the structural change is induced by the adsorbate. This suggests that in the presence of competing interactions these two tendencies are mixed to give qualitatively new structures.

The competing effects discussed above take place even if the substrate has the hexagonal symmetry. In this case the symmetry of a close packed adlayer is the same as that of the substrate. Then the effective radii a_{ij} are expected to induce stronger impact than that of the magnitudes V_{ij} . Let us recall that the short-ranged repulsing contribution with the magnitude V_{21} and the radius a_{21} was initially introduced to stabilize the numerical solution. Nevertheless the repulsing cores are always important in reality. The range of repulsion and its ratio to the lattice spacing depend on the nature of the substances forming the interface. By increasing the stabilizing a_{21} contribution we produce a delocalization of the adsorbate. This allows us to study cooperative effects arising due to the long-ranged coupling between the subsystems. In addition, we can investigate the configurations different from those favored by the strong localization condition accepted

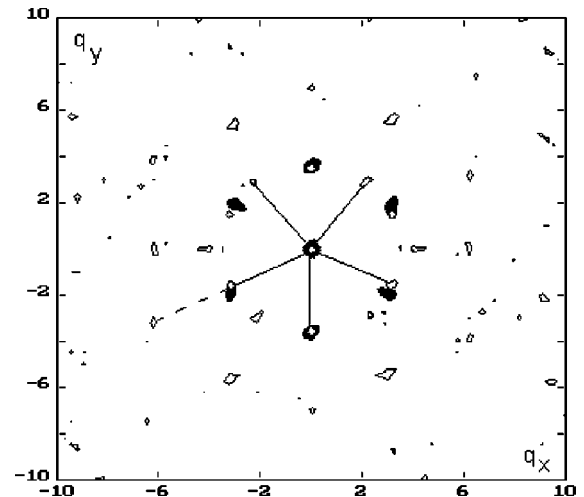


FIG. 9. Maxima of $G_{11}(\mathbf{q})$ for the substrate configuration shown in Fig. 8(a). Solid lines connect the pentagonal symmetry set in the first \mathbf{q} shell, the dashed line indicates some of such peaks in the next shell. All the quantities are dimensionless (see text).

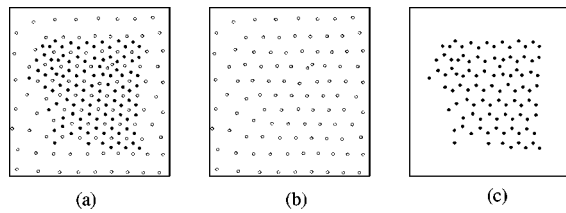


FIG. 10. The honeycomb adsorbate structure appearing at the hexagonal substrate with increasing range of attraction between the subsystems. The common configuration (a), the substrate (b), and adsorbate (c) configurations.

within the theoretical study. In particular, we set $V_{ij}=5, a_{21}=1.75, a_{11}=0.8, a_{22}=2.5, a_{12}=0.5$. The snapshots corresponding to this choice are shown in Fig. 8. The substrate (a) exhibits a distorted hexagonal structure, but the adsorbate (b) forms a pentagonal array. This is a cooperative effect appearing due to the coupling of an adsorbate particle to many substrate particles ($a_{22}=2.5$). The coupling results in an effective attraction between the adsorbates and favors a multiple bonding. Then some substrate sites remain “empty” [as is seen in (c)]. The encircled fragment represents a typical arrangement of pentagons at the hexagonal substrate. The empty substrate sites contribute to the distortions observed in the snapshot (a).

The substrate correlation function is shown in Fig. 9. Black peaks correspond to the unperturbed lattice (only the first \mathbf{q} shell is shadowed). In addition, two sets of the adsorbate-induced (pentagonal) peaks are observed within the same range of \mathbf{q} . One of these sets is indicated, the other may be visualized by symmetrical prolongation of the arms across the central peak. This indicates that the substrate acquires a pentagonal substructure due to the coupling with the adsorbate.

If we decrease the range of the substrate repulsion ($a_{11}=0.42$) and increase the range of attraction between the subsystems ($a_{12}=0.75$), then we observe a honeycomb adsorbate structure shown in Fig. 10(c). It is seen that the substrate

is almost unchanged (b). The common arrangement (a) is quite peculiar. In fact, each substrate site is a center of the adsorbate cell.

V. CONCLUSION

In this paper we have studied the influence of the adsorbate on the underlying substrate through the competing interaction between them.

Employing a generalized lattice gas theory and the BD simulation, we have shown that the competing displacive interaction in the adsorbate may cause a continuous distortive transition in the underlying substrate.

The threshold for the transition is determined by the competition of the substrate rigidity and the quasielastic energy induced by the adsorbate. The theoretical prediction (within the MFA) for the behavior of the order parameter agrees well with the simulation result.

In the presence of a strong pinning and repulsive lateral interaction, the resulting structure appears as a compromise between the square lattice of the substrate and the hexagonal arrangement of the adsorbate.

The difference of coverages for the distorted and undistorted lattices is determined by the average distortion energy. This difference is positive (negative) for attractive (repulsive) lateral interactions.

For hexagonal substrate lattices the simulation demonstrates that various adsorbate structures (from honeycomb lattices to quasicrystalline pentagonal configurations) may be observed, depending on the effective radii of interaction. Due to the long-ranged coupling the substrate correlation function may acquire additional maxima which reflect a substructure induced by the adsorbate.

ACKNOWLEDGMENTS

E.V.V. gratefully acknowledges financial support from the French Ministry of Education, Research and Technologies. For A.E.F. this work was supported in part within the CNRS Cooperation Program Ukraine-France.

-
- [1] B. N. J. Persson, *Surf. Sci. Rep.* **15**, 1 (1992).
 [2] J. Villain and M. B. Gordon, *Surf. Sci.* **125**, 1 (1983).
 [3] W. Steele, *Surf. Sci.* **36**, 317 (1973).
 [4] W. Selke, in *Phase Transitions and Critical Phenomena*, edited by C. Domb and J. Lebowitz (Academic Press, London, 1992), Vol. 15, p. 1.
 [5] A. D. Novaco and J. P. McTague, *Phys. Rev. Lett.* **38**, 1286 (1977); J. P. McTague and A. D. Novaco, *Phys. Rev. B* **19**, 5299 (1979).
 [6] M.-C. Desjonqueres and D. Spanjaard, in *Concepts in Surface Physics*, edited by D. Spanjaard, Springer Series in Surface Sciences Vol. 30 (Springer-Verlag, Berlin, 1993).
 [7] S. Titmuss, A. Wander, and D. A. King, *Chem. Rev.* **96**, 1291 (1996).
 [8] V. P. Zhdanov and P. R. Norton, *Langmuir* **12**, 101 (1996).
 [9] V. P. Zhdanov and B. Kasemo, *J. Chem. Phys.* **108**, 4582 (1998).
 [10] V. P. Zhdanov and B. Kasemo, *Phys. Rev. B* **56**, R10067 (1997).
 [11] E. D. Resnyanskii, E. I. Latkin, A. V. Myshlyavtsev, and V. I. Elokhin, *Chem. Phys. Lett.* **248**, 136 (1996); E. D. Resnyanskii, A. V. Myshlyavtsev, V. I. Elokhin, and B. S. Bal'zhinimaev, *ibid.* **264**, 174 (1997).
 [12] H. Ibach, *Surf. Sci. Rep.* **29**, 193 (1997).
 [13] J. E. Müller, M. Wuttig, and H. Ibach, *Phys. Rev. Lett.* **56**, 1583 (1986).
 [14] W. Daum, C. Stuhlmann, and H. Ibach, *Phys. Rev. Lett.* **60**, 2741 (1988).
 [15] A. Grossmann, W. Erley, J. B. Hannon, and H. Ibach, *Phys. Rev. Lett.* **77**, 127 (1996).
 [16] P. Fenter, A. Eberhardt, and P. Eisenberg, *Science* **266**, 1216 (1994); N. Camillone III, T. Y. B. Leung, and G. Scoles, *Surf. Sci.* **373**, 333 (1997).
 [17] M. Lindroos, H. Pfnür, G. Held, and D. Menzel, *Surf. Sci.* **222**, 451 (1989).
 [18] E. V. Vakarin, A. E. Filippov, and J. P. Badiali, *Phys. Rev. Lett.* **81**, 3904 (1998).

- [19] E. V. Vakarin, A. E. Filippov, and J. P. Badiali, *Surf. Sci.* **422**, L200 (1999).
- [20] J. P. Badiali, L. Blum, and M. L. Rosinberg, *Chem. Phys. Lett.* **129**, 149 (1986).
- [21] D. A. Huckaby and L. Blum, *J. Chem. Phys.* **92**, 2646 (1990); **97**, 5773 (1992).
- [22] L. Blum, *Adv. Chem. Phys.* **78**, 171 (1990).
- [23] M. L. Rosinberg, J. L. Lebowitz, and L. Blum, *J. Stat. Phys.* **44**, 153 (1986).
- [24] G. A. Baker, Jr. and J. W. Essam, *Phys. Rev. Lett.* **24**, 447 (1970); *J. Chem. Phys.* **55**, 861 (1971).
- [25] H. Wagner, *Phys. Rev. Lett.* **25**, 31 (1970); *H. Wagner, Z. Phys.* **239**, 182 (1970).
- [26] L. Gunther, D. J. Bergman, and Y. Imry, *Phys. Rev. Lett.* **27**, 558 (1971); D. J. Bergman and B. I. Halperin, *Phys. Rev. B* **13**, 2145 (1976).
- [27] E. Vives and A. Planes, *Phys. Rev. A* **41**, 1885 (1990).
- [28] N. W. Ashcroft and N. D. Mermin, *Solid State Physics* (Holt, Rinehart and Winston, New York, 1976).
- [29] R. Blinc and B. Zeks, *Soft Modes in Ferroelectrics and Antiferroelectrics* (North-Holland, Amsterdam, 1974).
- [30] R. A. Cowley, *Adv. Phys.* **29**, 1 (1980).
- [31] A. D. Bruce, *Adv. Phys.* **29**, 111 (1980).
- [32] M. P. Allen and D. J. Tildesley, *Computer Simulation of Liquids* (Oxford Science Publications, Clarendon Press, Oxford, 1994).
- [33] B. N. J. Persson, *Phys. Rev. Lett.* **71**, 1212 (1993); *Phys. Rev. B* **48**, 18 140 (1993).
- [34] F.-J. Elmer, *Phys. Rev. E* **50**, 4470 (1994); M. Weiss and F.-J. Elmer, *Phys. Rev. B* **53**, 7539 (1996).
- [35] M. G. Rozman, M. Urbakh, and J. Klafter, *Phys. Rev. Lett.* **77**, 683 (1996); *Phys. Rev. E* **54**, 6485 (1996); *Europhys. Lett.* **39**, 183 (1997).
- [36] O. M. Braun, T. Dauxois, M. V. Paliy, and M. Peyrard, *Phys. Rev. Lett.* **78**, 1295 (1997); *Phys. Rev. E* **55**, 3598 (1997).
- [37] M. Paliy, O. Braun, T. Dauxois, and B. Hu, *Phys. Rev. E* **56**, 4025 (1997).
- [38] O. M. Braun, A. R. Bishop, and J. Röder, *Phys. Rev. Lett.* **79**, 3692 (1997).
- [39] L. D. Landau and E. M. Lifshitz, *Statistical Physics* (Pergamon, London, 1958).
- [40] V. P. Zhdanov, J. L. Sales, and R. O. Unac, *Surf. Sci.* **381**, L599 (1997).